Energy, Mines and Resources Canada | Énergie, Mines et Ressources Canada

CANMET

Canada Centre for Mineral and Energy Technology | Centre canadien de la technologie des minéraux et de l'énergie

PERFORMANCE OF MAGNESIA-CARBON BRICKS IN VACUUM AT HIGH TEMPERATURE

D.H.H. Quon and K.E. Bell
Mineral Processing Laboratory

June 1986

Project: 30.29.05
Electrodes and Refractories for Steelmaking

This document is an unedited draft report prepared primarily for discussion and review purposes. It does not represent final opinion of the division of the Canada Centre for Mineral and Energy Technology (CANMET)

Ce document est un rapport préliminaire non-révisé et rédigé principalement aux fins de discussion et de documentation interne. Il ne représente nullement l'opinion définitive de la division du Centre canadien de la technologie des minéraux et de l'énergie (CANMET)

39 pp

MINERAL SCIENCES LABORATORIES
DIVISION REPORT MSL 86-83 (IR)

AUG 19 1986

MICROMEDIA

PERFORMANCE OF MAGNESIA-CARBON BRICKS IN VACUUM AT HIGH TEMPERATURE

by

D.H.H. Quon* and K.E. Bell**

ABSTRACT

The chemical-structural profiles of four types of MgO-C bricks with 15 to 24% carbon in contact with three different types of slag at temperatures of 1650 and 1700°C in vacuum were examined. Retardation of slag penetration owing to the presence of graphite was demonstrated. The corrosion resistance of the MgO is strongly dependent on the slag composition and increases with the basicity of the slag. In vacuum at 1700°C, extensive loss of components by vaporization was recorded. This loss by vaporization/sublimation was augmented by reduction of MgO in contact with graphite to Mg, which was deposited in the cooler parts of the furnace, thus opening up further surface area to slag corrosion.

The corrosion resistance of a fused cast chrome-magnesia block was also examined. By virtue of its greater density/lower porosity, the fused cast material shows little volatilization into vacuum at high temperature, compared with both rebonded fused grain chrome-magnesia and MgO-C bricks. The slag resistance decreases with increasing temperature.

---

*Research Scientist and **Head, Ceramic Section, Mineral Processing Laboratory, Mineral Sciences Laboratories, CANMET, Energy, Mines and Resources Canada.

PERFORMANCE DES BRIQUES DE MAGNÉSIE-CARBONNE CHAUFFÉES SOUS VIDE À UNE TEMPÉRATURE ÉLEVÉE

par

D.H.H. Quon* et K.E. Bell**

RÉSUMÉ

Les profils chimiques et structurals de quatre types de briques MgO-C contenant de 15 à 24 % de carbone, en contact avec trois différents genres de laitiers, chauffées sous vide à des températures variant de 1 650 à 1 700°C, ont été étudiés. Le retardement de la pénétration du laitier en raison de la présence du graphite a été démontré. La résistance du MgO à la corrosion dépend principalement de la composition du laitier et s'accroît en fonction de la basicité de celui-ci. Quand les briques sont chauffées sous vide à une température de 1 700°C, une perte importante de composantes par évaporation est enregistrée. Cette perte résultant de l'évaporation-sublimation s'est accrue par la réduction de MgO, en contact avec du graphite, à Mg qui s'est déposé sur les parties les plus froides de la chaudière exposant ainsi une plus grande surface à la corrosion.

La résistance à la corrosion d'un bloc de chrome-magnésie fondu et coulé à également été étudiée. En raison de sa grande densité et d'une porosité plus faible, le matériau fondu et coulé à démontré peu de volatilité comparativement aux briques de chrome-magnésie réagglomérées et aux briques de MgO-C, lorsque chauffé sous vide à une température élevée. La résistance du laitier a diminuée proportionnellement à l'augmentation de la température.

---

*Chercheur scientifique et **Chef, Section de la céramique, Laboratoire de traitement des minéraux, CANMET, Énergie, Mines et Ressources Canada.

INTRODUCTION

Magnesia-carbon (MgO-C) bricks have been used successfully in converter linings since 1978. Their use has become well established in electric arc furnace hot spots, and they have been used in non-hot spot wall areas and at the slagline since 1980 (1,2). The use of such special refractories in the more vulnerable parts of the furnace lining makes it possible to attain uniform wear over-all, thus increasing service life and reducing refractories consumption. The reported advantage of MgO-C bricks lies in the high slag corrosion resistance of the carbon component.

Magnesia-carbon materials thus have potential for replacing the rebonded fused grain chrome-magnesia brick used at the slagline and the fused cast chrome-magnesia blocks used in the hot spots of secondary steelmaking vessels. The aim of this study is to evaluate the performance of MgO-C bricks in contact with secondary steelmaking slags in order to assess their applicability in vacuum vessels (VOD, VAD).

CHARACTERISTICS OF MAGNESIA-CARBON BRICKS

The MgO-C bricks are composed principally of carbon and magnesia. Compositionally, these bricks are relatively simple but can be increasingly complexed by altering the C/MgO ratio, type of carbon, type of magnesia and type of bond. The carbon level in the brick can be varied from as low as 4% to as high as 30%. Mikami and Martinet (3) classified these bricks into four different categories according to the carbon content as follows:

1) 4-5% class - used principally in the basic oxygen furnace or converter;
2) 8% class - extensively used in electric arc furnace in the U.S.A.;
3) 13% class - including carbon levels from 12 to 16%;
4) 18-25% class - the highest carbon level is nominally about 20% to as high as 30%. Extensively used in electric arc furnaces in Japan.

In addition to the carbon level in the brick, the characteristics of the carbon can be varied. The carbon may be composed of flake graphite, carbon black, amorphous carbon and petroleum coke, and may be bonded to the magnesia by pitch or resin. The magnesia grains are present in the brick either as sintered grains, fused-grains and/or a combination of the two.

Use of MgO-C refractories in basic oxygen furnaces has been discussed by several investigators (3-19). Herron et al. reported that a carbon content of at least 3% is required to minimize slag migration into the brick structure (5). Pickering and Batchelor indicated that the carbon and magnesia are thermodynamically incompatible under steelmaking conditions at about 1600°C (14). Both weight and strength loss occurred as a result of the reduction of magnesia and oxidation of the carbon, which produced extensive microstructural change. The existence of a dense zone at or near the hot face of the brick, resulting from the reduction of the MgO and vaporization of Mg, with subsequent reoxidation and precipitation of MgO results in an improvement in the slag resistance of the refractories as indicated by Baker et al. (10). However, not all other workers have been able to confirm the existence of such a dense zone.

EXPERIMENTAL

MATERIALS

Materials used for this study were supplied by the Atlas Steels Company, Welland, Ontario. A list of the various types of unused MgO-C bricks and their physical and chemical properties is given in Table 1. In addition to the unused bricks, samples of used MgO-C brick and rebonded fused grain chrome magnesia bricks were obtained from the electric arc furnace for the study. Slag resistance of an unused fused cast chrome-magnesia block manufactured by the Cohart Company was also evaluated for comparison with the MgO-C bricks.

MICROSCOPY

Polished sections of the used, unused and laboratory-tested unused bricks were prepared. The microstructures of these refractories were characterized using both optical and scanning electron microscopy (SEM). Semi-quantitative analysis of the compositional change of used and test bricks resulting from the interaction with different slags at high temperatures was determined using energy dispersive X-ray analysis (EDXR).

SLAG RESISTANCE TEST

The slag resistance of the bricks was conducted in a high temperature vacuum furnace. The test procedure (cup-test) is described elsewhere (2). The slag compositions used for the tests are given in Table 2.

RESULTS

MICROSTRUCTURE OF USED MAGNESIA-CARBON BRICK (NO. 6)

Megascopically, the used brick #6 from the electric-arc furnace shows only a very narrow zone of slag-brick interface. The SEM micrograph in Fig. 1 shows this slag-brick interface, where the reaction of the slag and brick to form a calcium silicate phase is indicated by the Ca and Si distribution maps obtained by EDXR. The Mg and Al distribution maps indicate that, in this narrow zone, the MgO from the brick reacts at high temperature with the alumina from the slag to form a spinel phase. The adjacent periclase grains are surrounded by the flake graphite, which protected them from slag corrosion.

MICROSTRUCTURES OF THE UNUSED MAGNESIA-CARBON BRICKS

The graphite content of the magnesia-carbon bricks for this study varied from 14.7 to 24%.

The major visible difference megascopically in these bricks is the colouration of the grog grains, which are yellowish for samples 6 and 7 and white for 8A and 8B.

The optical micrographs in Fig. 2 show the microstructures of the unused bricks. Generally, they are composed of large periclase grog grains in a fine-grained groundmass of periclase and flake graphite. Sample 8A, in addition to the grog grains, contains also periclase single crystals.

An SEM micrograph of sample 6, as received, reveals that the grog grains are composed of fine periclase grains that are bonded by calcium silicate at the grain boundaries (Fig. 3). Flake graphite occurs principally in the groundmass and at the boundaries of the grog grains. Another phase was detected in the groundmass: it contains impurities such as Cr, Al and Fe crystallized in the form of spinel.

The microstructure of sample 7 (unused) is shown in Fig. 4 to be very similar to the microstructure of brick 6. However, the secondary phase material is comprised of Mg and Al, as determined by EDXR, crystallized in the form of magnesia-alumina spinel.

The SEM micrograph and elemental distribution maps for Ca, Mg and Si for sample 8A (unused) given in Fig. 5 shows that the finer grained periclase is bonded by calcium silicate to form the grog grains. In the groundmass, in addition to the periclase and flake graphite, quartz was also detected. The EDXR analysis also showed that minor amounts of Fe, K, Al, S and P are present, and that these impurities are associated with the graphite flakes.

An SEM micrograph and elemental distribution maps of Mg, Ca, Si, Fe and S for sample 8B (unused) are given in Fig. 6. The periclase grog grains are composed of very fine grained periclase bonded together by calcium silicate. In the interstices, phases such as calcium silicate and iron sulphide were detected. These and all the principal impurities are associated with the graphite flakes, as evidenced by another section, shown in Fig. 7 along with elemental distribution maps for Mg, Ti, Al, Fe and Si, where an alumina-titania-silica occlusion in the graphite is shown, as well as lesser iron silicate impurities.

MICROSTRUCTURE OF THE USED AND UNUSED CHROME-MAGNESIA BRICKS

The used rebonded fused grain chrome-magnesia brick from the electro-arc furnace is dark brown, containing an 8 mm wide light gray slag impregnated zone with scattered metal droplets. SEM micrographs of the three distinct zones developed in the used brick are given in Fig. 8 to 10. The slag brick interface is composed of recrystallized subhedral to anhedral spinel and metal droplets (Fig. 8). In the slag zone, the microstructure and elemental distribution maps for Ca, Mg and Al are given in Fig. 9, revealing that anhedral spinels were crystallized in the calcium aluminate slag. Behind the slag brick interface, the microstructure can be seen in Fig. 10a. In this case, the chrome spinel crystals are distributed randomly in the periclase matrix, with some of the periclase being rimmed by the chrome spinel. Another typical texture also observed includes randomly distributed anhedral spinel grains in the periclase matrix, as illustrated in Fig. 10b. These local variations in texture have been noted previously and attributed to the manufacturing process (2).

The unused fused cast chrome-magnesia block is darker brown. The microstructures of the block are given in Fig. 11a and 11b. A gradual change of the grain size of the periclase grains containing an exsolved spinel phase is shown in Fig. 11a. This characteristic reflects the crystallization behaviour during the fabrication of the brick. A higher cooling rate occurred at the surface of the brick, which is responsible for the development of the small periclase and spinel crystals. In contrast, the large periclase grains, containing exsolved blebs of spinel and rimmed by spinel, to be found in the interior indicate that the cooling rate of the melt was sufficiently slow to allow such a texture to develop.

CORROSION RESISTANCE OF MAGNESIA-CARBON REFRACTORIES

Three types of slags having calcium to silica (C/S) ratios varying from 1.35 to 3.54 were used to test the corrosion resistance of these bricks at high temperature in vacuum.

Magnesia-Carbon Bricks in Contact with C/S = 1.35 Slag

In contact with the slag at 1650°C for 3 h, microcracks were developed in samples 6, 7 and 8B. The slag either partially or completely penetrated into the test cup. A tendency for solidified slag to decrepitate in the test cup was observed on cooling to room temperature, due to the inversion of the polymorphic dicalcium silicate. To properly characterize the slag-brick interface, SEM microscopy was used.

The microstructure and elemental distribution of Ca, Mg and Si at the slag-brick interface for sample 6 is given in Fig. 12. The slag corrosion is restricted to a narrow zone, principally in the fine-grained periclase groundmass.

The microstructure of sample 7 in contact with the slag is shown in Fig. 13. The slag corrosion is restricted to the grain boundaries of the periclase grog grains and graphite flakes. EDXR maps for Ca, Mg, Si and Al reveal that calcium alumino-silicates crystallized around the periclase grains (Fig. 13). A similar microstructure and slag corrosion characteristic at the slag-brick interface was also observed in sample 8A as shown in Fig. 14. The principal phases developed at the reaction zone are solid solutions of the calcium alumino-silicates.

Magnesia-Carbon Bricks in Contact with C/S = 3.13 Slag

Both samples 8A and 8B were in contact with this slag at 1700°C for 1.5 h only, as mass vaporization loss of Mg was observed and the volatile condensed in the optical windows and made temperature measurement and control ineffective.

An SEM micrograph and EDXR maps for Mg, Al, Ca, and Si of sample 7 in contact with the VAD slag are given in Fig. 15. The principal phases, calcium silicate and calcium aluminosilicates, crystallized at or near the periclase grog grains.

In contact with slag for 1 h at 1700°C, the microstructures of samples 8A and 8B at the slag-brick interface are given in Fig. 16 and 17 respectively. The corrosion characteristics of these two bricks are identical: in both, the slag infiltration followed the partings of the flake graphite and along the contacts between the graphite and the periclase grains. Based on the elemental distribution maps for Ca, Mg, Si and Al, the phases crystallized are calcium silicate and calcium aluminosilicates.

Magnesia-Carbon Refractories in Contact with C/S = 3.54 Slag

In contact with slag having C/S = 3.54 at 1650°C for 3 h, vaporization loss of Mg was observed. The rate of vaporization loss is greater for samples 8A and 8B than for samples 6 and 7. This was indicated by the amount of Mg crystals deposited in the cooler part of the vacuum furnace chamber.

The microstructure and elemental distribution of Ca, Mg and Si at the slag-brick interface of sample 6 are shown in Fig. 18. In contact with slag, the MgO crystals have dissolved and reacted with the calcium and silica to form a rim of calcium magnesium silicate around the periclase grains. The distribution of the calcium silicate, as outlined by the EDXR map for Ca and Si, indicates that the slag also penetrated along the cleavages of the graphite.

The microstructure and elemental distribution of Ca, Mg, Si and Al at the slag-brick interface for sample 7 reveals that the slag infiltrated mainly along the contact between the graphite and periclase grains, and along the grain boundaries of the grog grains as indicated by the presence of calcium aluminum silicates (Fig. 19).

The SEM micrograph and EDXR maps for Ca, Mg, Si and Al of sample 8B at the slag-brick interface are given in Fig. 20. Calcium-magnesium-aluminum silicate forms reaction rims on the periclase grog grains. The penetration of slag follows grain boundaries or along the contact between the graphite and the periclase grog grains.

Volatilization Loss of Magnesium From the Magnesia-Carbon

In vacuum, substantial amounts of MgO loss occurred in the brick due to the periclase grains being in contact with the carbonaceous material. The reaction may be represented by the following equation:

$$MgO(s) + C(s) \longrightarrow Mg(g) + CO(g)$$

The above reaction is particularly noticeable at 1700°C, where Mg vapor was condensed in the cooler part of the vacuum chamber. Attempts were made to determine the amount of MgO loss versus time relative to graphite content of the refractories at 1700°C. However, a systematic correlation was not found, due perhaps to the non-uniform distribution of the periclase grains and also the manner in which these two materials were in contact with one another; i.e., the total weight loss is probably a function of variations in both the amounts of MgO vaporization and of decarbonization. The weight loss results obtained are given in Table 4, for heating at a constant rate to the temperatures indicated. Tests on samples 6 and 8A had to be suspended at 1650°C, when vapours condensed on the pyrometer sight parts and furnace control became uncertain.

CORROSION RESISTANCE OF FUSED CAST CHROME-MAGNESIA

Fused Cast Chrome-Magnesia in Contact with C/S = 1.35 Slag

Microstructure and elemental distribution maps of Ca, Si and Fe for the fused cast chrome magnesia brick in contact with the low C/S slag are given in Fig. 21. At a temperature of 1650°C for 3 h, the depth of slag penetration is about 40 μm and in this zone the principal phase is dicalcium silicate.

Fused Cast Chrome-Magnesia Brick in Contact with C/S = 3.54 Slag

The microstructure of the fused-cast chrome magnesia brick in contact with high C/S slag at 1700°C for 3 h is given in Fig. 22. Based on the elemental distribution maps of Ca and Si, also in the figure, a slag zone of about 80 μm was developed in the brick, which is much wider than for the same brick in contact with the low C/S slag at 1650°C for 3 h.

Volatilization Loss of Magnesia From the Fused Cast Chrome-Magnesia Brick

Volatilization loss of MgO from the rebonded fused grain chrome-magnesia brick at high temperature in vacuum has been reported by several investigators (1,2). Test results of the MgO loss in vacuum at 1700°C for the fused cast brick varied between 0.43 and 0.6% /h, which is substantially less than that of the carbon magnesia brick (Table 4). It is also significantly less (about half) of that previously determined for rebonded fused grain chrome- magnesia, attributed to lower initial porosity (less exposed surface area) of the fused cast material.

DISCUSSION AND CONCLUSIONS

Degradation of MgO-C bricks at high temperatures in vacuum appears to involve the continuous removal of a thin superficial layer at the hot face in contact with slag. The presence of the graphite inhibits penetration at depth of the slag, owing to its non-wetting properties. Hence, loss of refractory materials proceeds by:

1) direct chemical corrosion of the MgO by the slag; restricted to exposed surfaces but proceeds somewhat more rapidly at the less-resistant grain boundaries, particularly where silicates and other impurities are present. The rate of attack is higher with less-basic slags (low Ca/Si ratios) and increases with increasing temperature. It can also be expected to be directly related to bulk density and open porosity, which would provide increased surface area for reaction;

2) vaporization of constituents into vacuum at high temperatures; has been shown previously for MgO, and graphite is well-known to sublime, at least to some extent, at the temperatures in question. The carbon would also be prone to oxidation, either during oxygen blowing or by direct reduction of oxides in contact. For example, the loss of both components is exacerbated by reaction between MgO and C to form gaseous Mg and CO, demonstrated in the cup tests where the resultant channels between MgO and graphite grains were penetrated by slag. The weight loss studies indicate that vaporization probably becomes excessive at temperatures above 1700°C. Again, as vaporization is a surface phenomenon, it would be directly related to open porosity.

In non-vacuum environments such as BOF service, other investigators (10,11,14) have shown the MgO-graphite reaction to be beneficial, attributed to re-oxidation of the gaseous Mg in the pores at the surface of the brick to form a highly dense, thin surface layer that reduces the surface area subject to both slag attack and vaporization. No such layer was found in any of the tests conducted at CANMET, leading to the conclusion that the gaseous Mg is removed completely under vacuum.

3) the modified and weakened surface layer may be eroded away by the strongly agitated metal and slag. This could not be demonstrated in the static cup tests employed.

Of the four Mg-C brick examined, samples 8A and 8B might be expected to be less resistant than their counterparts, samples 6 and 7. Microstructural examination indicated that the former contain more deleterious impurities in the grains and grain boundaries, both in terms of silicate phases and multiple minor impurities present, particularly in the graphite flakes (presumably natural graphite vs. synthetic material in samples 6 and 7). The presence of these impurities in the grain boundaries would form a liquid phase at high temperatures and render the grains more susceptible to subsequent erosion.

A subsidiary advantage reported for MgO-C bricks, in addition to their slag resistance, is their improved resistance to spalling by thermal shock. The usual explanation given is their high thermal conductivity, which reduces thermal gradients and hence thermal stresses, but probably also

involves absorption of stress within the somewhat resilient graphite flakes. Recently, investigators have reported upon the importance of the graphite distribution and pore structure in these products. No major differences in this respect were observed in the four samples examined at CANMET (cf. Fig. 2).

The fused cast chrome-magnesia block is highly slag resistant compared with the rebonded fused grain chrome-magnesia brick, as would be expected from its high density (low porosity) and the more uniform distribution of the spinel phase (which protects the MgO from attack). The same physical properties result in low vaporization loss into vacuum at high temperatures, compared with both rebonded fused grain chrome-magnesia and magnesia-carbon materials. Based on this performance, the fused cast chrome-magnesia would be preferred to either of the other materials for use in vacuum environments, although consideration must be given to cost and its lesser resistance to thermal shock.

ACKNOWLEDGEMENTS

The writers wish to express their thanks to G. Lemieux, Y. Bourgoin and D. Owens of CANMET for their contribution to this work. Thanks are also due to Atlas Steels Company for supplying the necessary materials for this study.

REFERENCES

1. Orlov, V.A., Sokolov, A.N., Polonskii, Ya. G., Mezetsev, E.P., Simonov, K.V., Kabonov, V.S., Suvoror, S.A., Kuznetsov, G.I., Chermak, A. and Gavlik, V. "New refractories for plant handling the vacuum treatment of steel outside the furnace"; Refractories (Translation from Russian Ogneupory) 21:67-80; 1980.
2. Quon, D.H.H. and Bell, K.E. "Degradation of slagline chrome magnesite bricks in secondary steelmaking under vacuum"; INTERCERAM. 2:50-52; 1983; 3:40-42; 1983.
3. Mikami, H.M. and Martinet, J.R. "Carbon-magnesia bricks in electric arc furnace"; Refract J 6:25-32; 1980.
4. Nacamu, R.L. and Lalama, S.J. "High carbon-magnesia refractories in basic oxygen steelmaking"; Refract J 4:9-14; 1982.
5. Herron, R.H., Beechan, C.R. and Padfield, R.C. "Slag attack on carbon-bearing basic refractories"; Bull Am Ceram Soc 46:1163-1168; 1967.
6. Park, H.K. and Barrett, L.R. "The corrosion resistance of carbon-containing magnesia refractories in melts"; Trans Br Ceram Soc 78:90-95; 1979.
7. Park, H.K. and Barrett, L.R. "The oxidation of carbon under melts"; Trans Br Ceram Soc 78:26-33; 1979.
8. Nacamu, R.L. and Batchelor, J.D. "Carbon oxidation as a function of BOF Brick texture"; Bull Am Ceram Soc 54:647-649; 1975.
9. Cooper, C.F. "Graphite containing refractories"; Refract J 2:11-21; 1984.
10. Baker, B.H., Brezny, B. and Shultz, R.L. "The role of carbon in MgO refractories"; Bull Am Ceram Soc 54:665-666; 1975.
11. Leonard, R.J. and Herron, R.H. "Significance of oxidation-reduction reactions within BOF refractories"; Bull Am Ceram Soc 55:1-10; 1972.
12. Lester, M. and Cooper, S.C. "The effect of carbon content, testing temperature and furnace atmosphere on the strength of tar-bonded and tar impregnated magnesite refractories"; Trans Br Ceram Soc 75:12-22; 1976.

13. Carniglia, S.C. "Limitations on the internal oxidation-reduction reactions in the BOF refractories"; Bull Am Ceram Soc 52:160-165; 1973.
14. Pickering, G.D. and Batchelor, J.D. "Carbon-MgO reactions in BOF refractories"; Bull Am Ceram Soc 50:611-614; 1971.
15. Marr, R.J. and Treffner, W.S. "Microstructure of periclase and carbon in BOF refractories"; Bull Am Ceram Soc 51:582-587; 1972.
16. Knoche, M., Koltermann, M. and Stolte, G. "Refractories for vacuum steelmaking"; Trans Br Ceram Soc 76:141-154; 1977.
17. Binns, D.B. "The use of special ceramics in handling molten iron and steel: a review"; Trans Br Ceram Soc 77:1-13, 1978.
18. Brezny, B. and Landy, R.A. "Microstructural and chemical changes of pitch impregnated magnesite brick under reducing conditions"; Trans Br Ceram Soc 71:163-170; 1972.
19. Evans, J.L. "Furnace design and operations-key to refractory performance"; Refract J 5:9-20; 1980.

Table 1. Chemical and physical properties of the MgO-C bricks

Brick No.	6	7	8A	8B
Name	Cardic	Cardic	PMT170EXAO	160PMTO
Composition				
MgO	71.8	72.0	73.2	82.0
C	24.0	18.3	23.8	14.7
Apparent porosity, %	3.5	3.5	4.4	4.0
Bulk density, kg/m	2850	2800	2760	2850
Supplier	N. American Refractories	N. American Refractories	Kyushu Refractories	Kyushu Refractories

Table 2. Compositions of the slags used for the cup test

	CaO	MnO	SiO_2	Cr_2O_3	Al_2O_3	MgO	C/S*
T1	44.8	-	33.3	0.6	10.5	9.81	1.35
VAD	60.06	0.06	19.2	0.02	10.11	3.69	3.13
VOD	60.12	0.10	17.0	0.02	7.68	4.27	3.54

*Weight ratio of CaO:SiO_2

Table 3. Observed behaviour of MgO-C bricks in cup tests

Sample No.	Slag Type			Temp. °C	Time h	Wt Loss %	Remarks
	T1	VOD	VAD				
6	x			1650	3	14.6	cc,sd
6		x		1650	3	18.5	mge,sd
6			x	1700	3		mge,sd
7	x			1650	3		cc,mge,sd
7		x		1650	3	30.0	--
7			x	1700	3		sd
8A	x			1650	3	19.6	sd,mge
8A		x		1650	1.5		mge
8A			x	1700	1.5	11.8	mge,sd
8B	x			1650	3	5.3	cc,mge,sd
8B		x		1650	1.5	34.0	sd
8B			x	1700	1.5	8.4	sd

**cc = cracks developed in crucible.
mge = Mg volatilized.
sd = decrepitation of residual slag inside the test crucible.

Table 4. Volatilization loss from MgO-C bricks

Sample No.	Temp. °C	Loss g/min
6	1650	0.86
7	1700	0.68
8A	1650	0.65
8B	1700	0.90

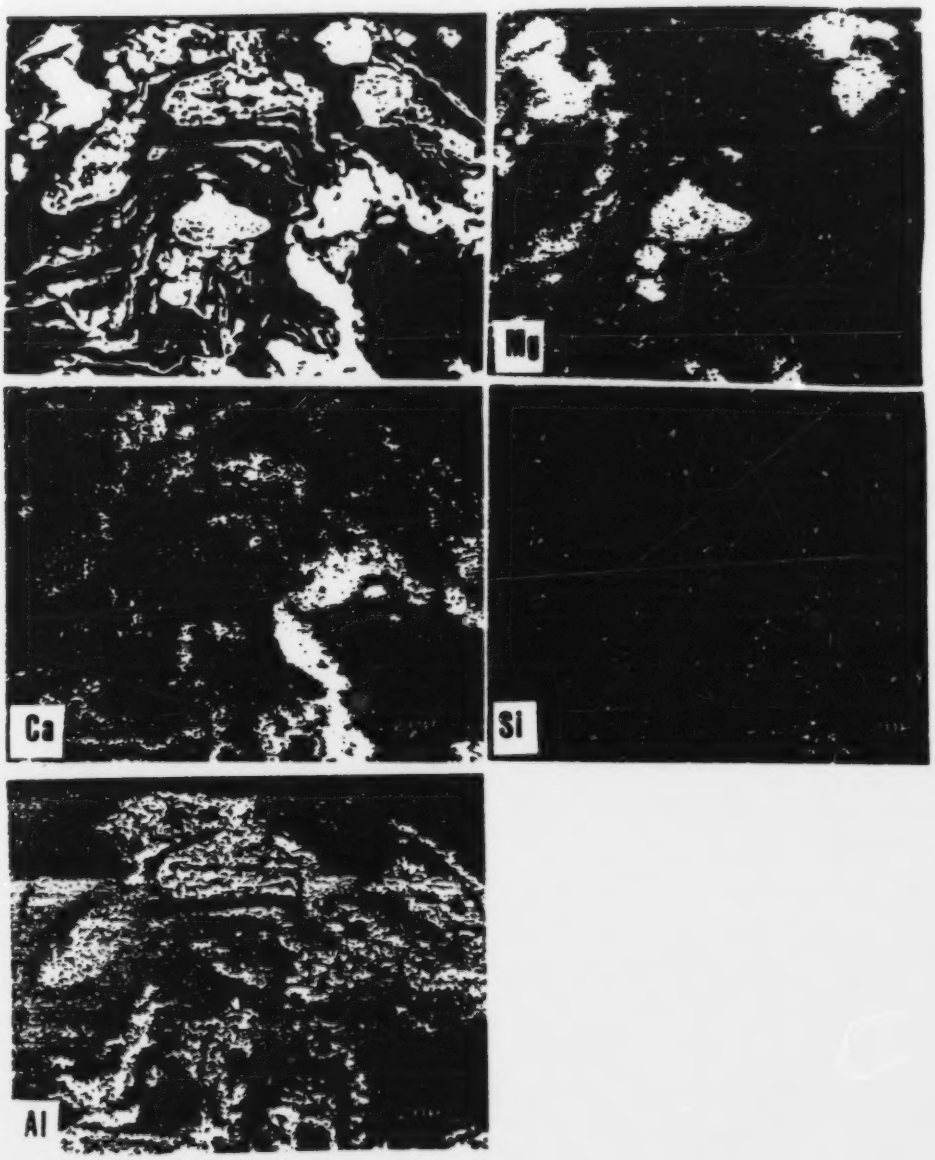

Fig. 1. SEM micrograph and elemental distribution maps of Mg, Ca, Si and Al for a used brick (sample 6) from the steel refining ladle

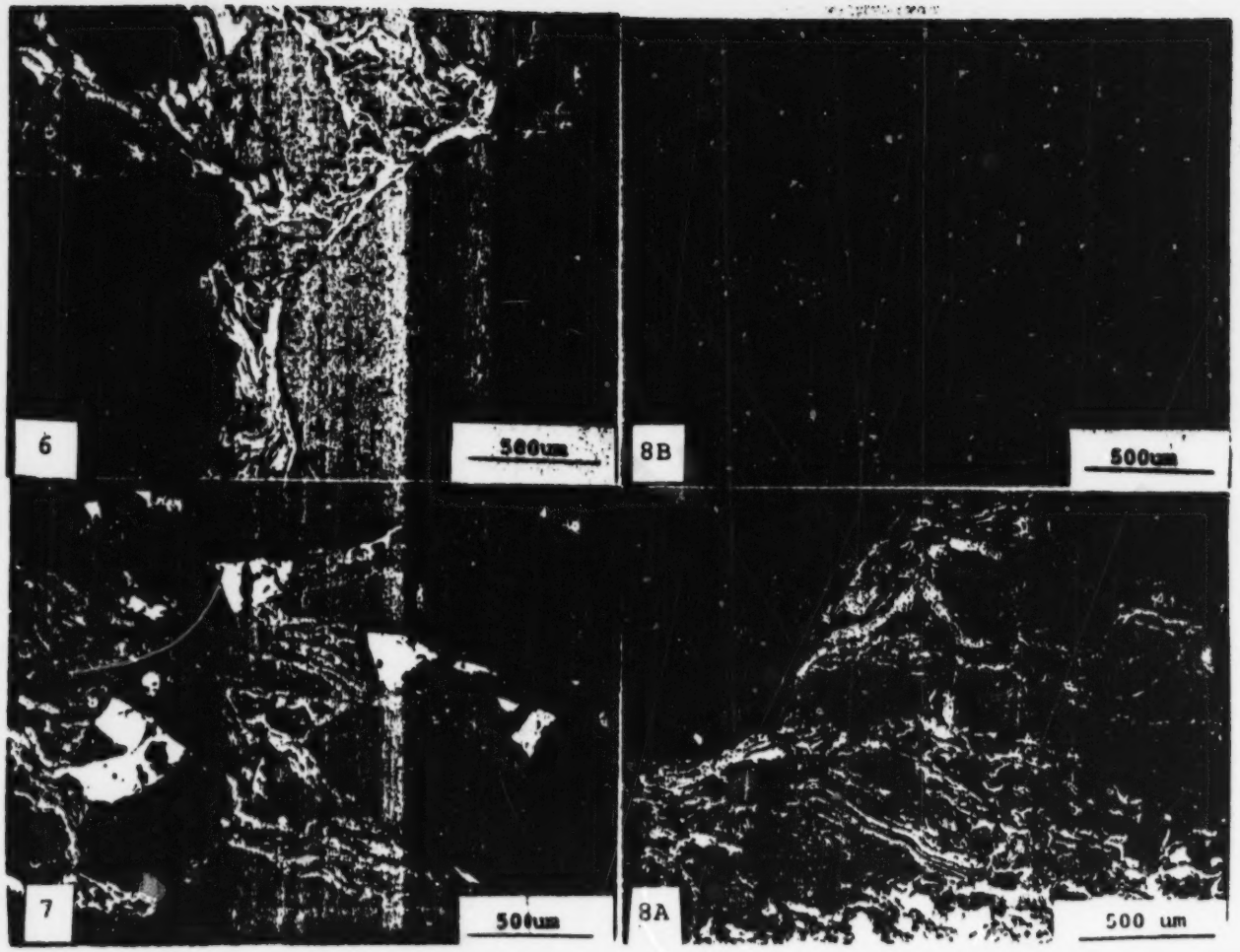

Fig. 2. Optical micrographs of the unused MgO-C bricks

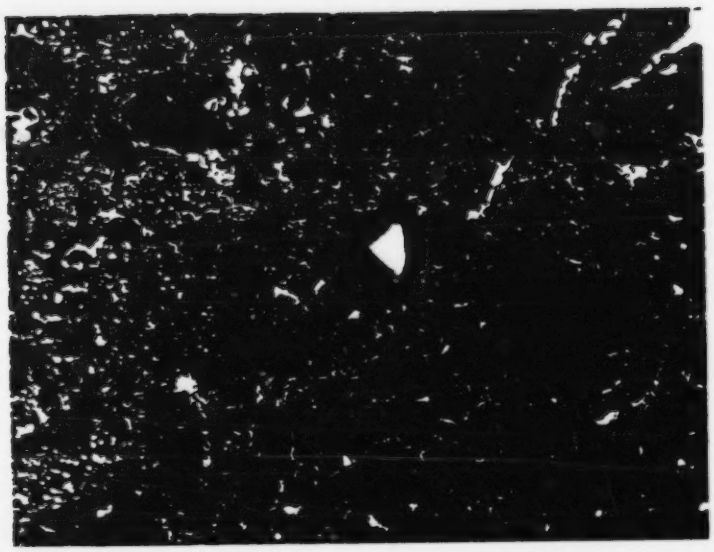

3a

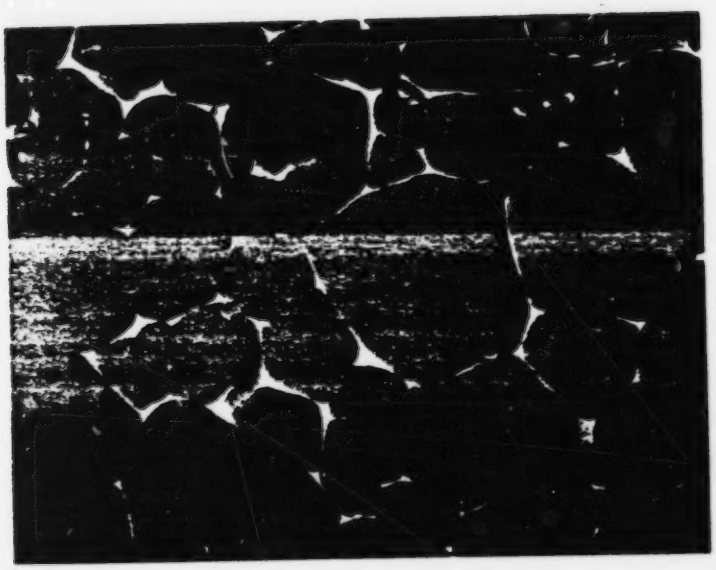

3b

Fig. 3. The microstructure of sample 6 (3a), and details of the calcium silicate formed at the grain boundaries of the periclase (3b)

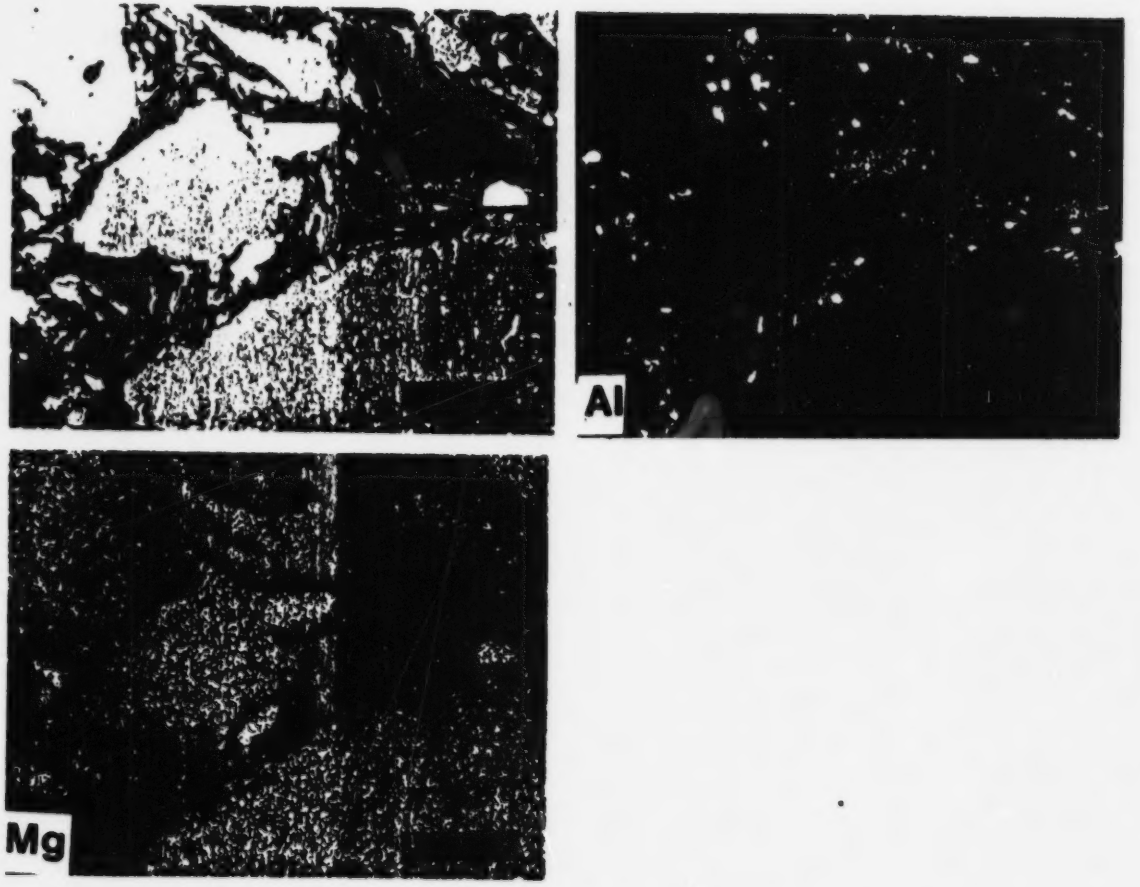

Fig. 4. SEM micrograph and elemental distribution maps of Mg and Al for sample 7

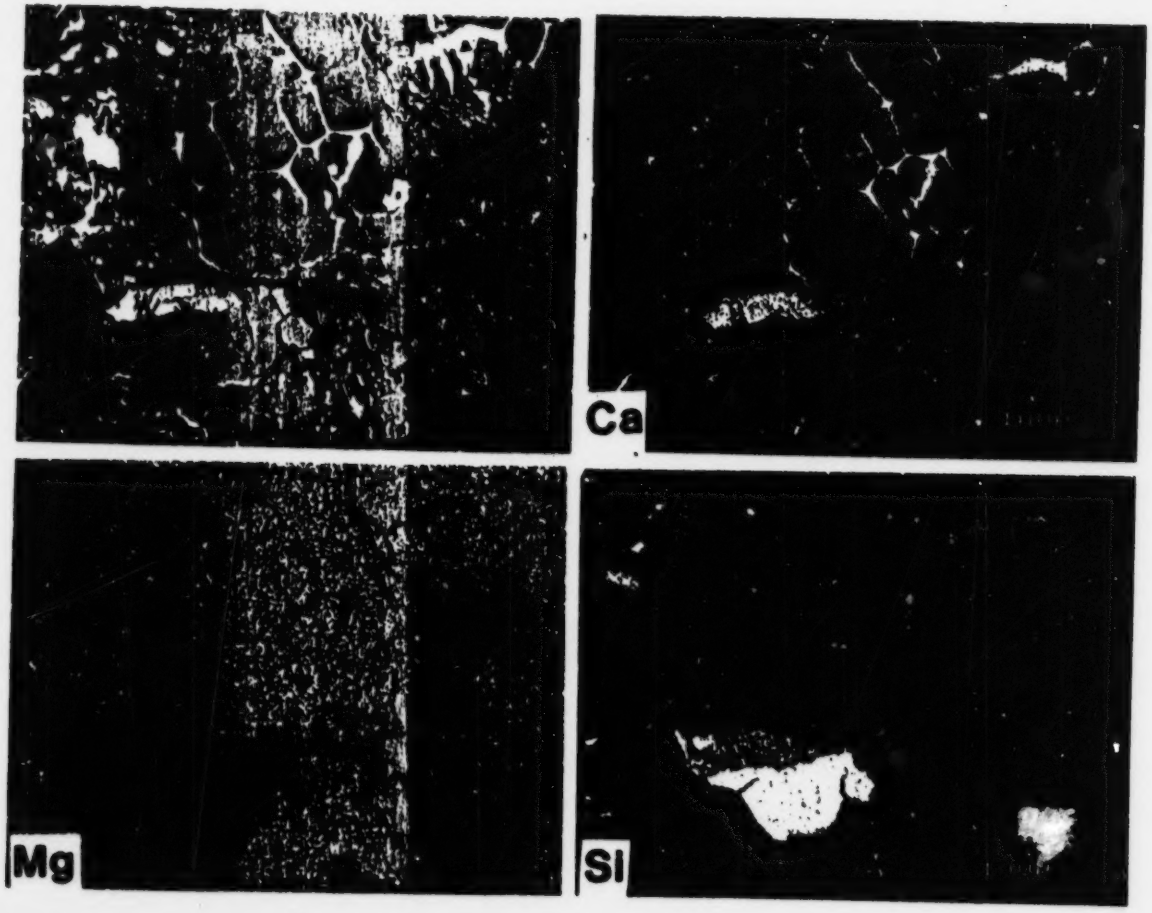

Fig. 5. SEM micrograph and elemental distribution maps of Ca, Mg and Si for sample 8A

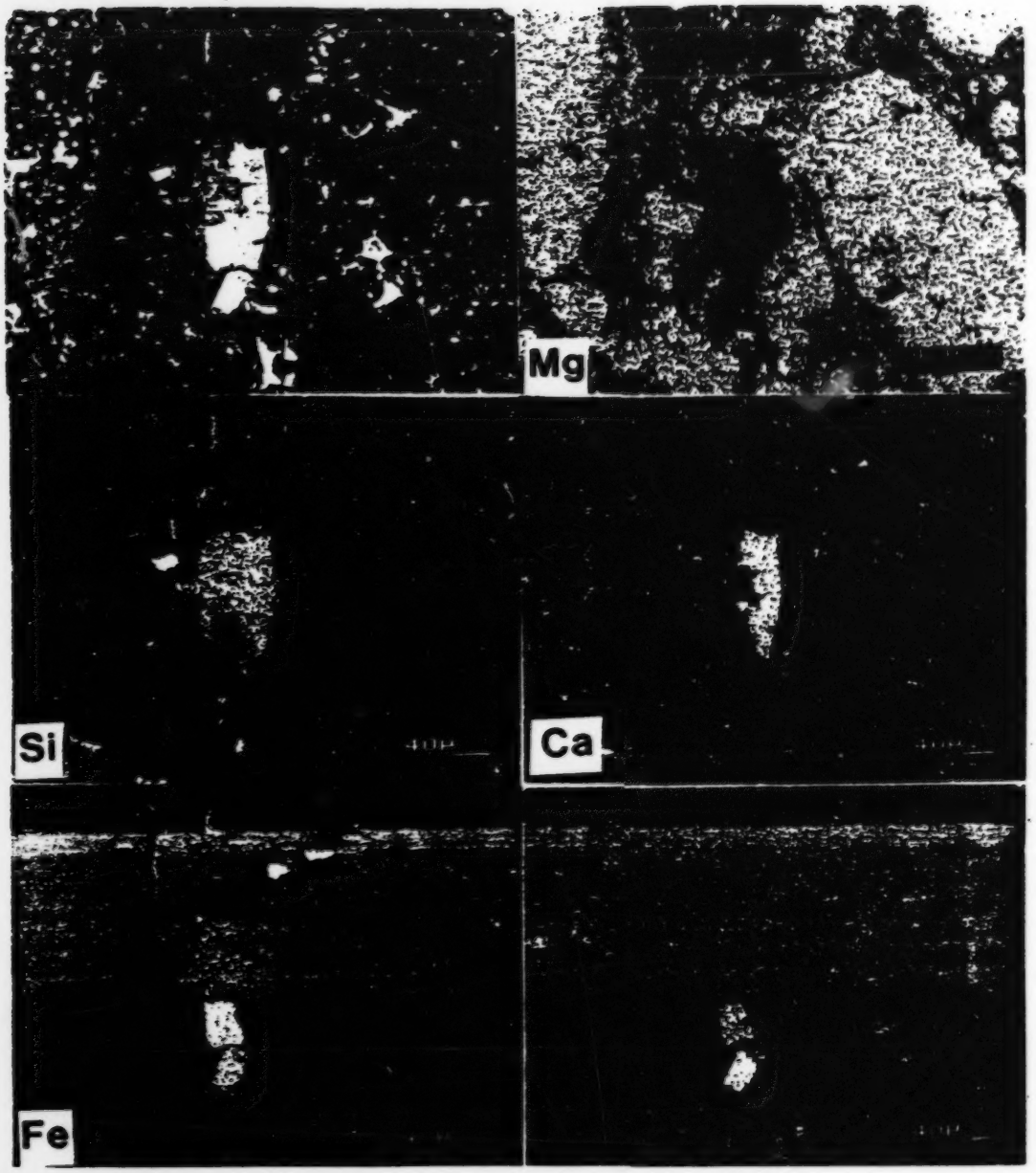

Fig. 6. SEM micrograph and elemental distribution of Mg, Ca, Si, Fe and S for unused brick, 8B

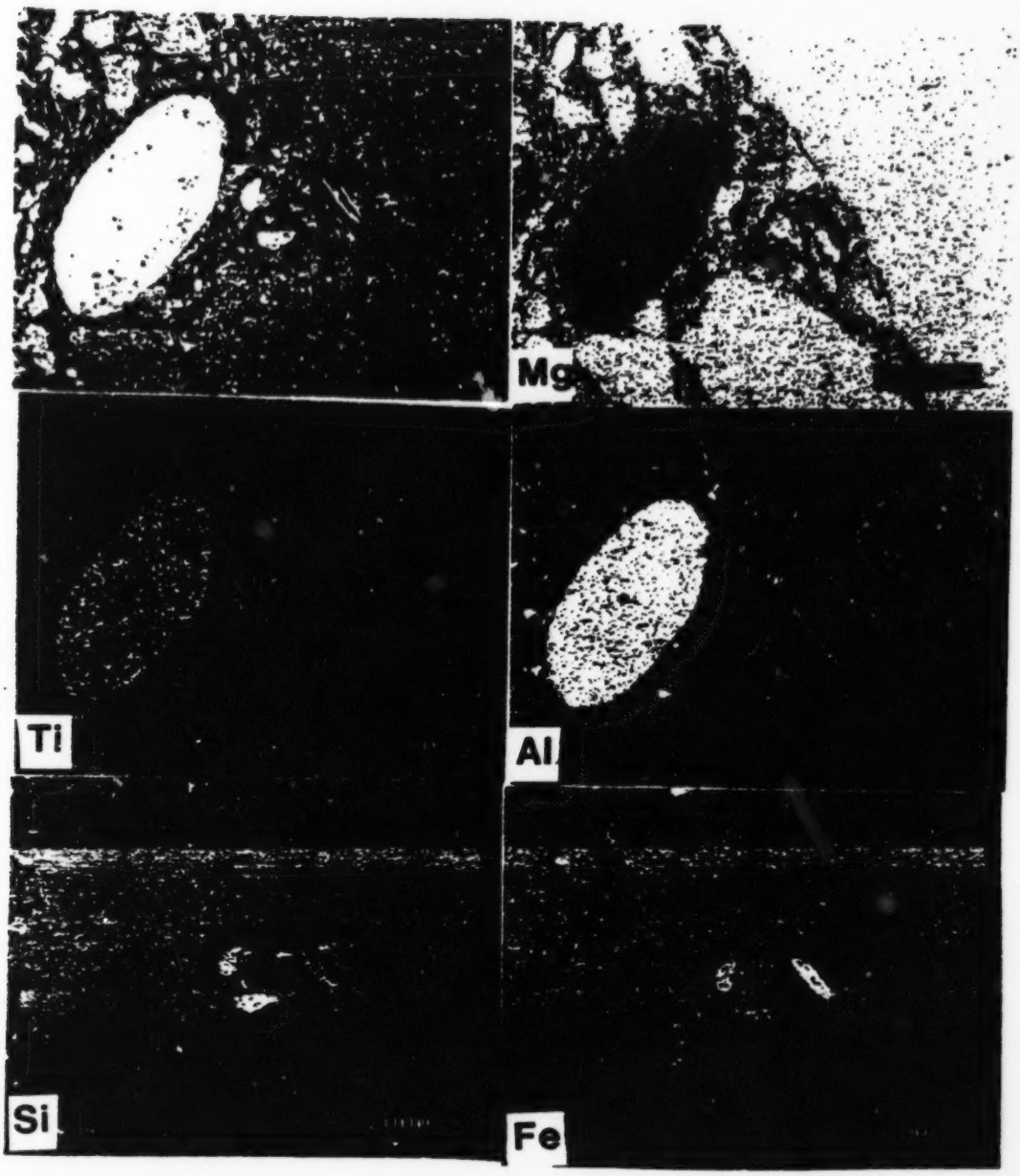

Fig. 7. SEM micrograph and elemental distribution maps of Mg, Ti, Al, Si, and Fe for unused bricks, 8B

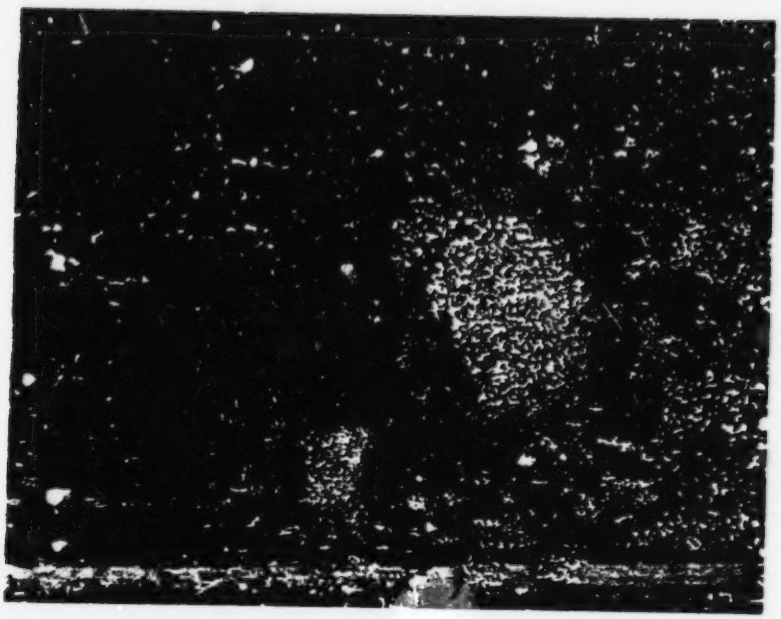

Fig. 8. SEM micrograph of slay-brick interface of a used rebonded fused grain chrome-magnesia brick

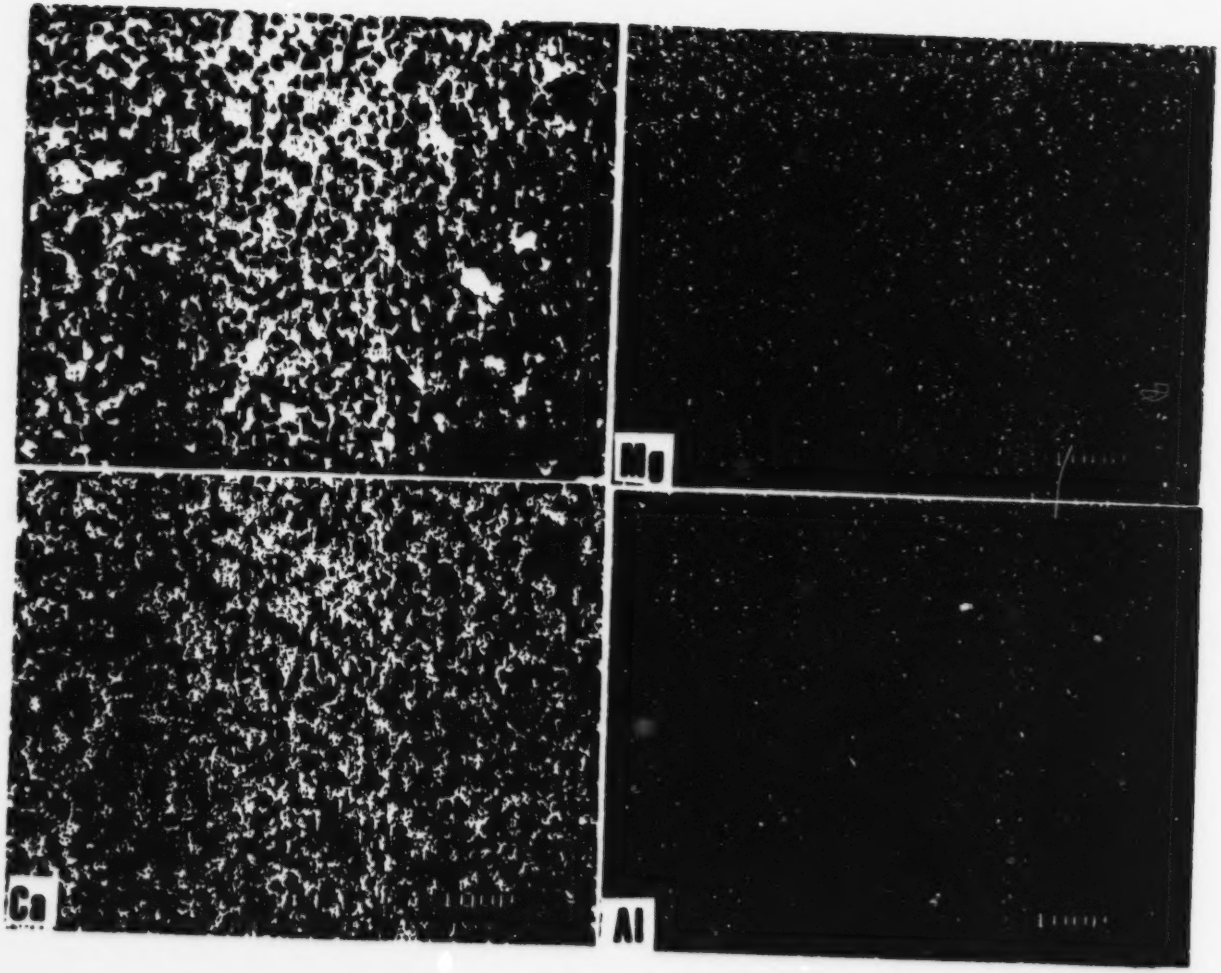

Fig. 9. SEM micrograph and EDXR maps for Ca, Mg and Al of a used rebonded fused grain chrome-magnesia brick of slag-brick interface

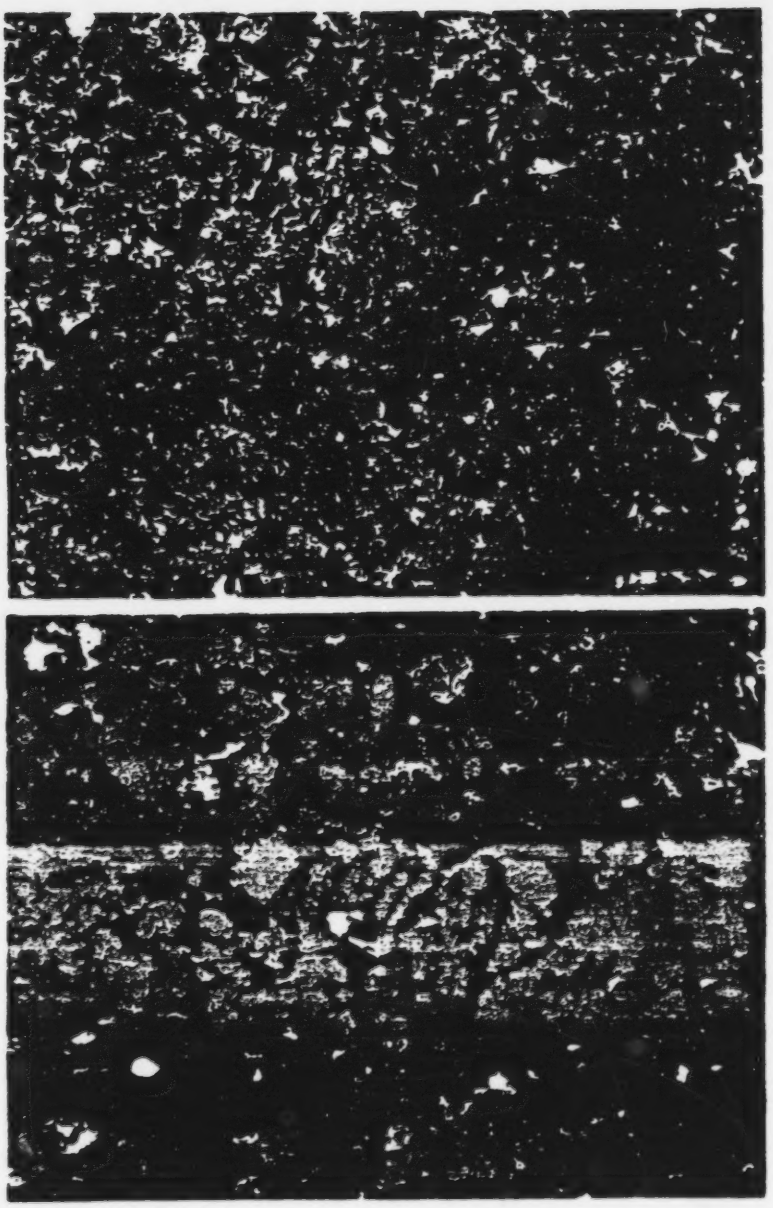

Fig. 10. SEM micrograph showing microstructures of a used rebonded fused grain chrome-magnesia brick behind the slag/brick interface

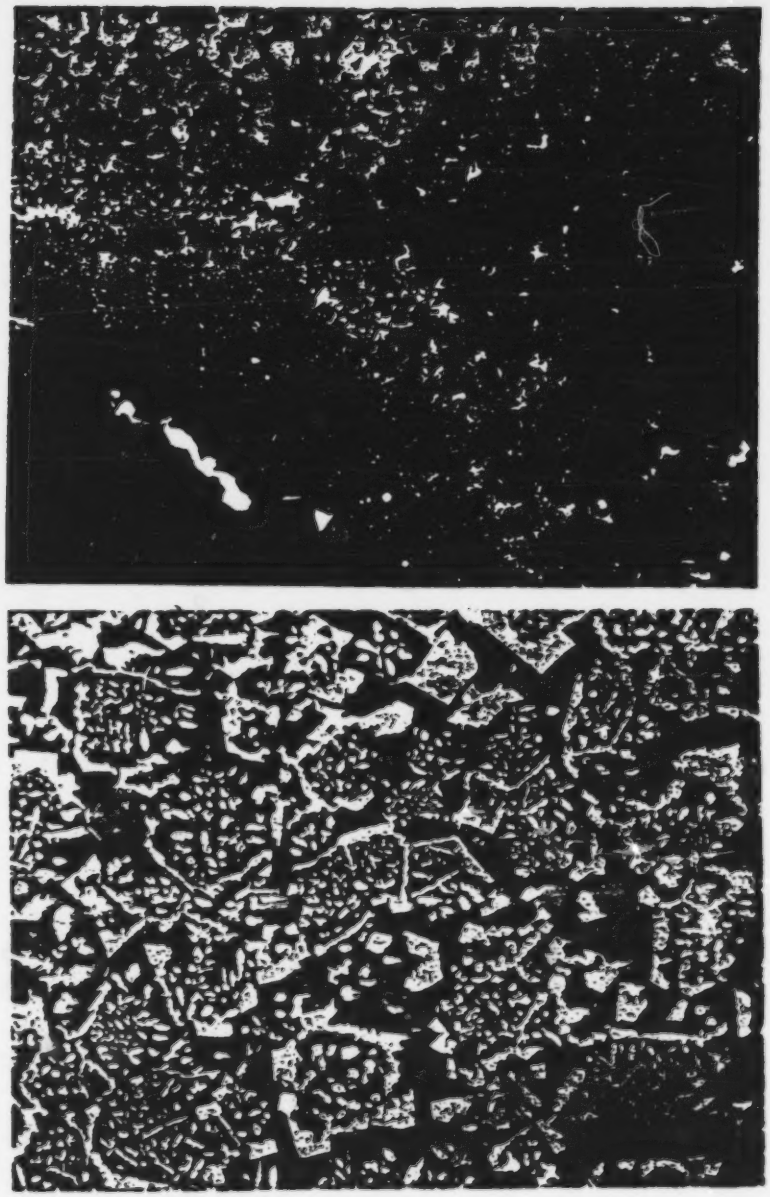

a

b

Fig. 11. Microstructures of the fused cast chrome-magnesia block, showing (a) the change in grain size with depth, and (b) typical microstructure, with chrome spinel dispersed within and rimming the periclase grains.

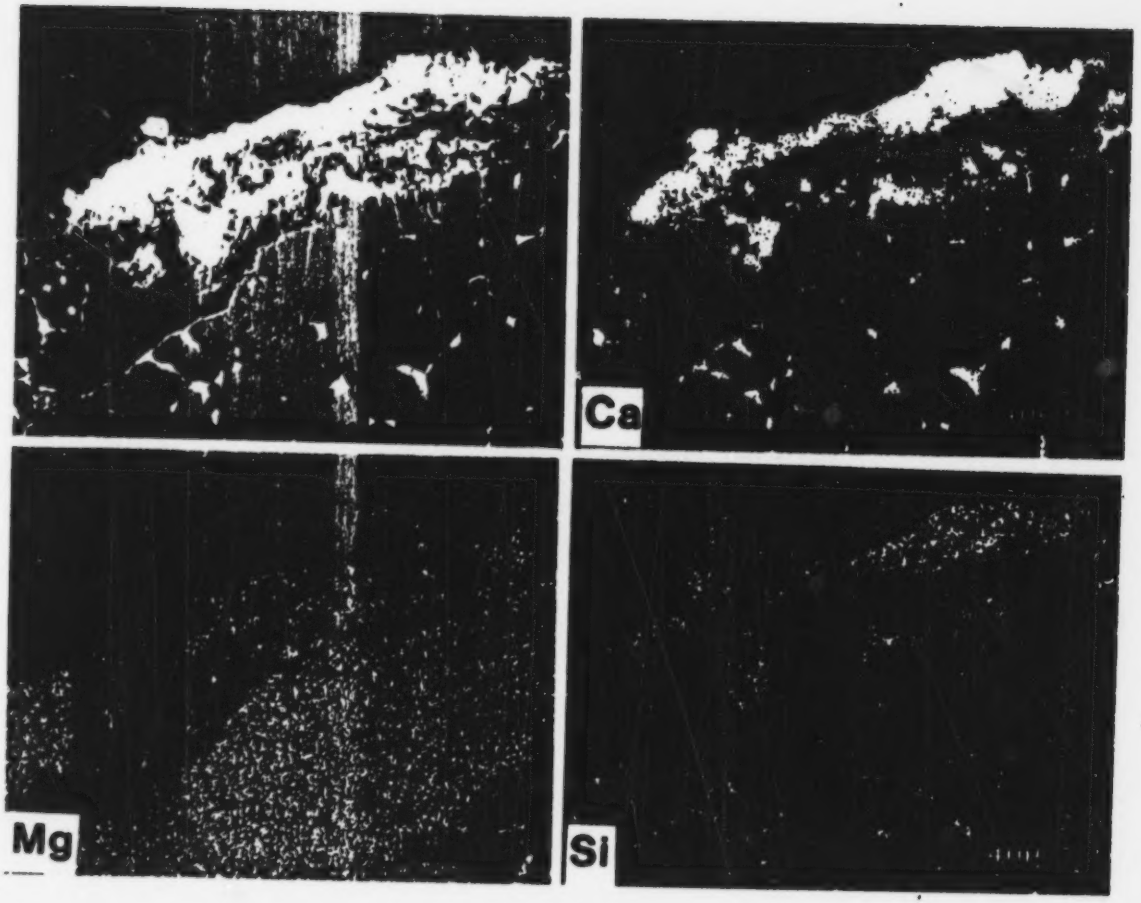

Fig. 12. SEM micrograph and elemental distribution of Ca, Mg and Si for MgO-C sample 6 in contact with slag having C/S ratio of 1.35

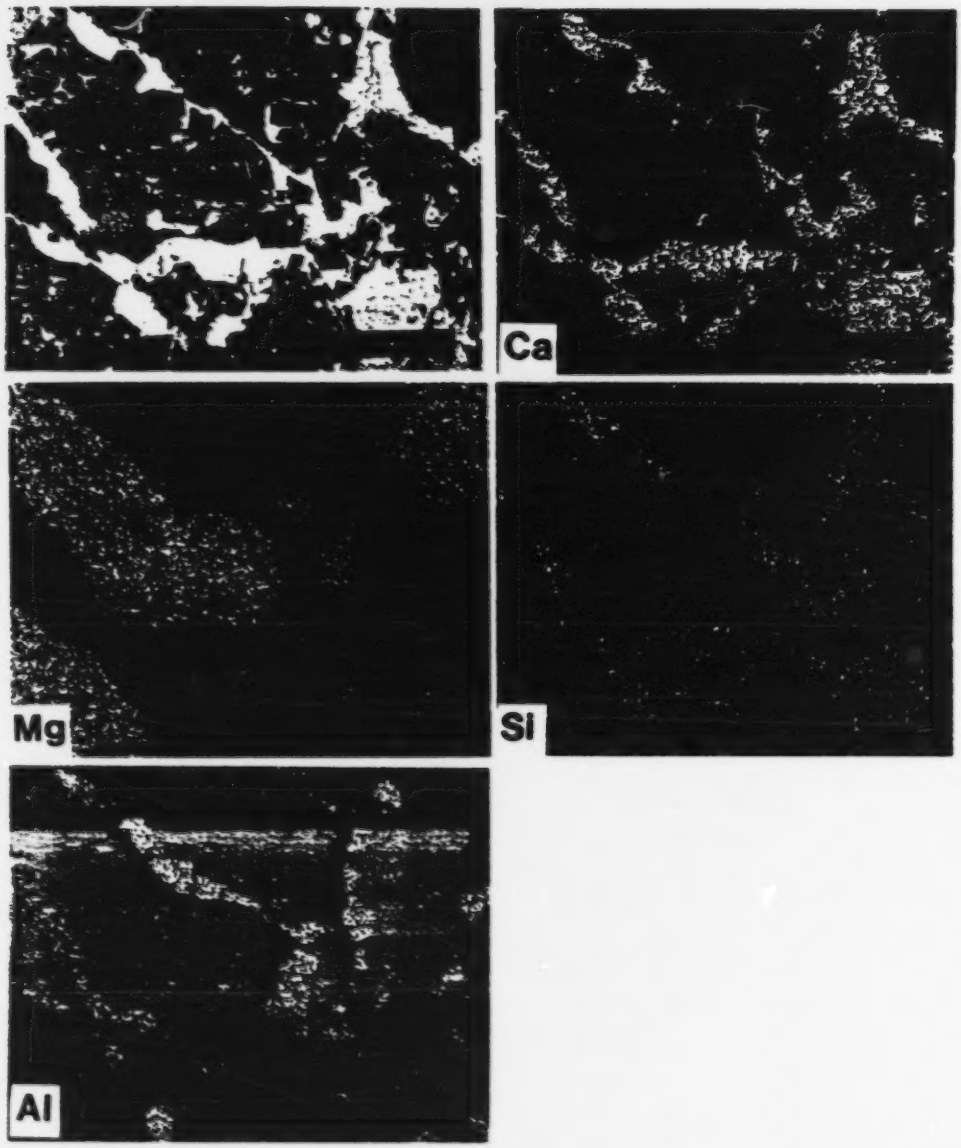

Fig. 13. SEM micrograph and elemental distribution maps of Ca, Si, Mg and Al for mgO-C sample 7 in contact with slag of C/S = 1.35

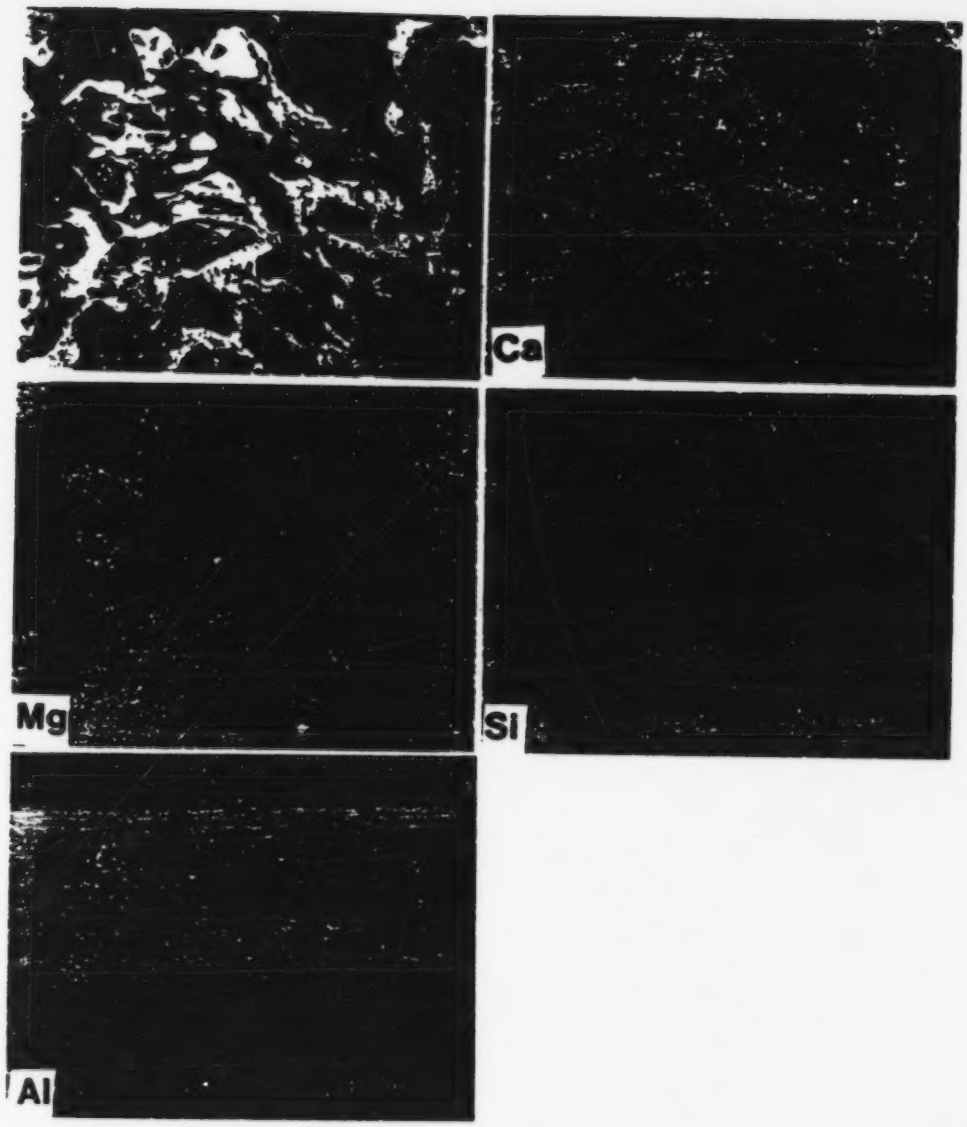

Fig. 14. SEM micrograph and elemental distribution maps of Ca, Mg, Si and Al for MgO-C sample 8A in contact with slag of C/S = 1.35

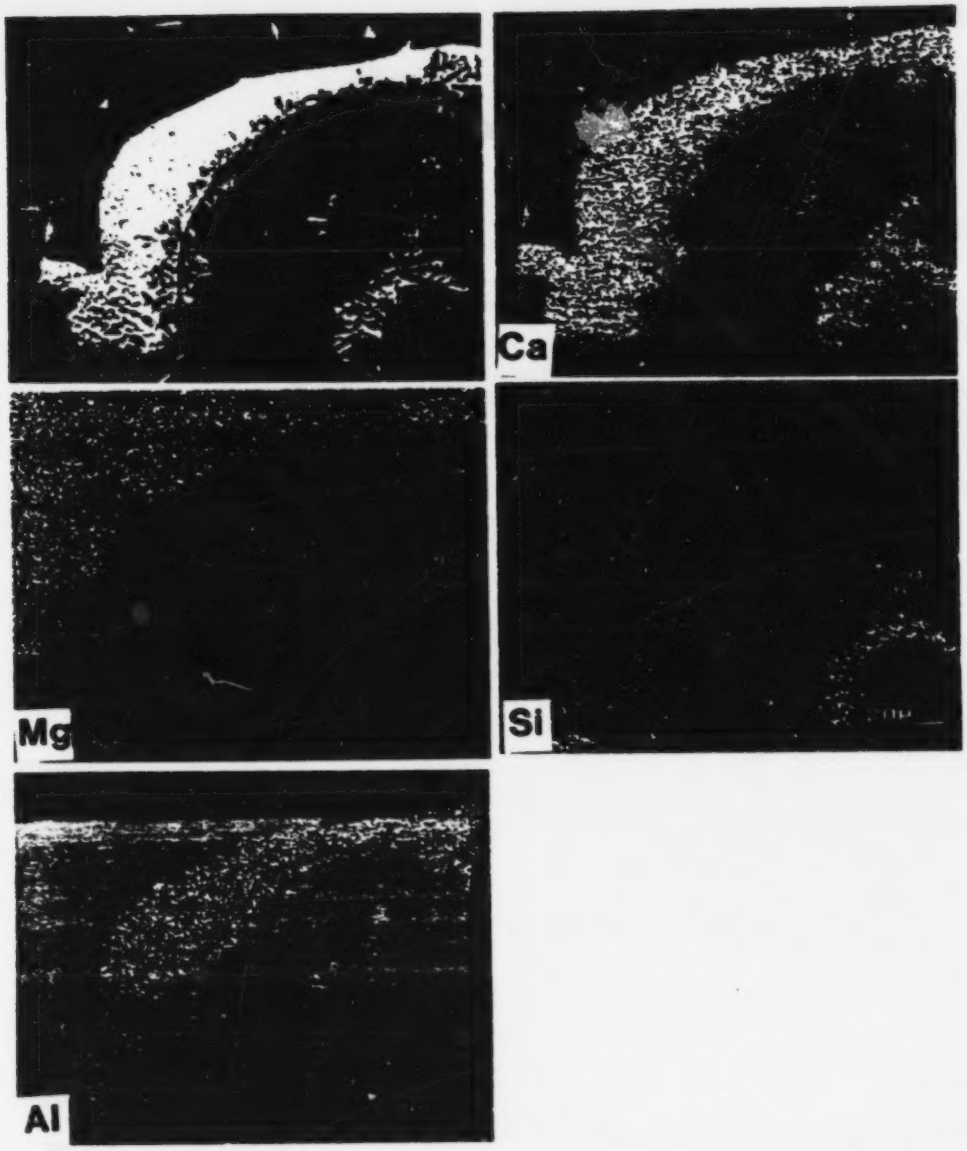

Fig. 15. SEM micrograph and elemental distribution maps of Ca, Mg, Si and Al for MgO-C sample 7 in contact with slag of C/S = 3.13

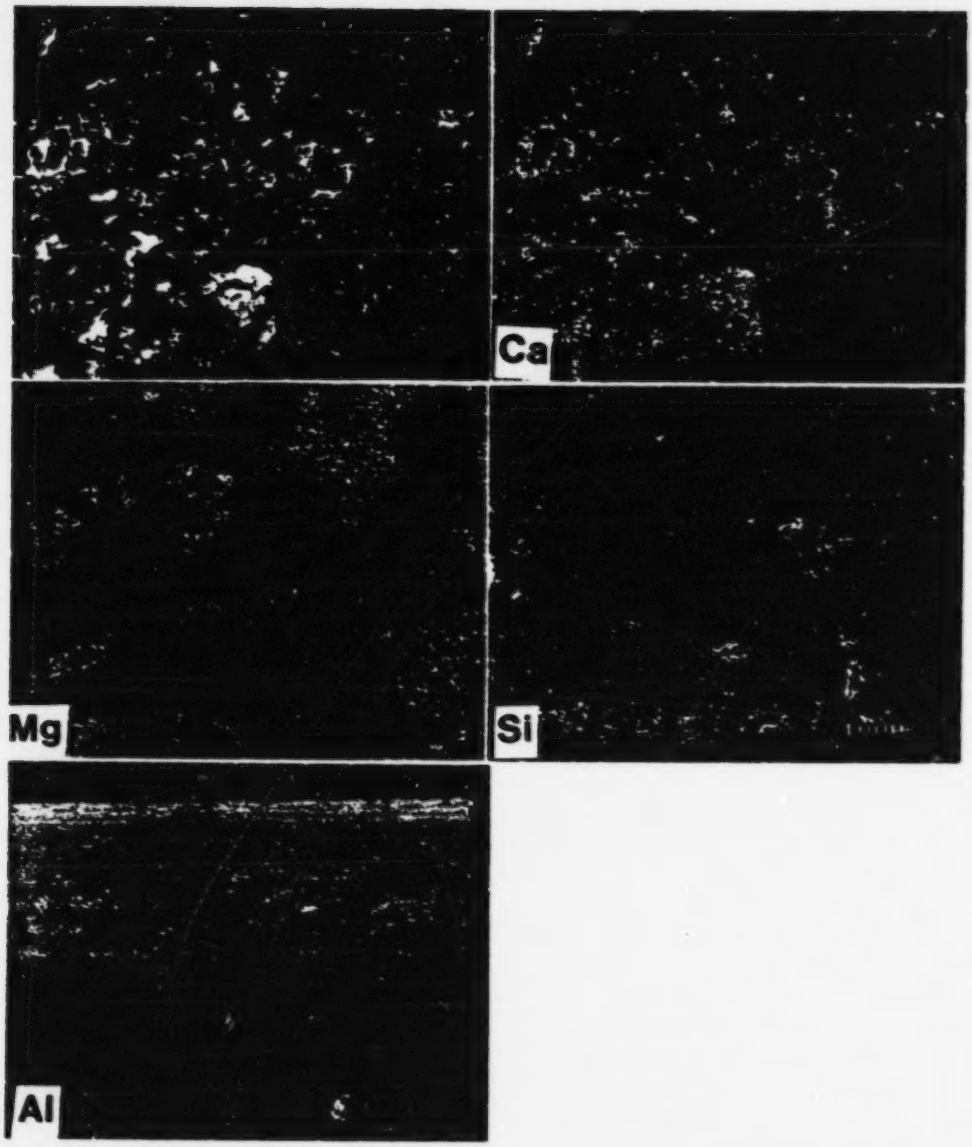

Fig. 16. SEM micrograph and elemental distribution of Ca, Mg, Si and Al of MgO-C sample 8A in contact with slag of C/S = 3.13

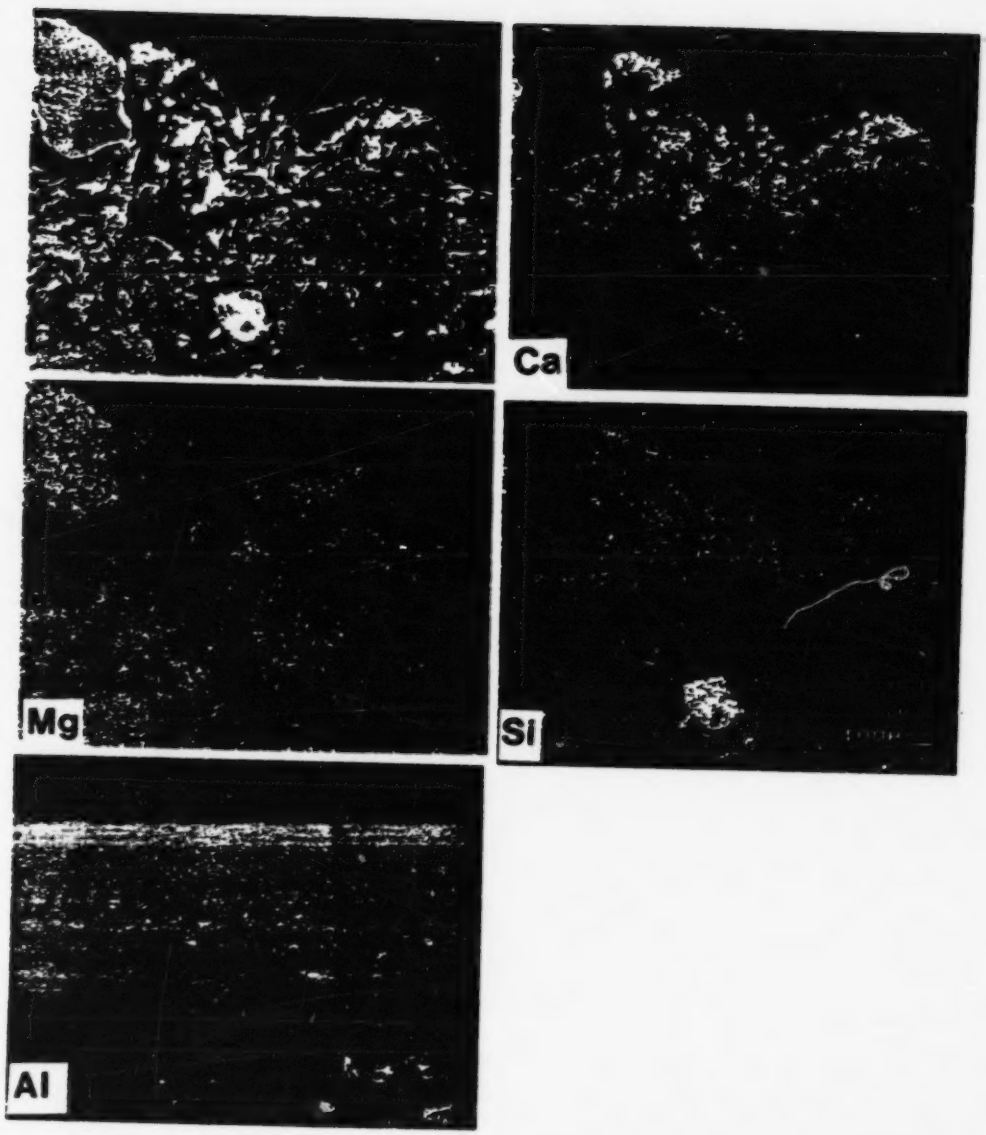

Fig. 17. SEM micrograph and elemental distribution maps of Ca, Mg, Si and Al for MgO-C sample 8B in contact with slag of C/S = 3.13

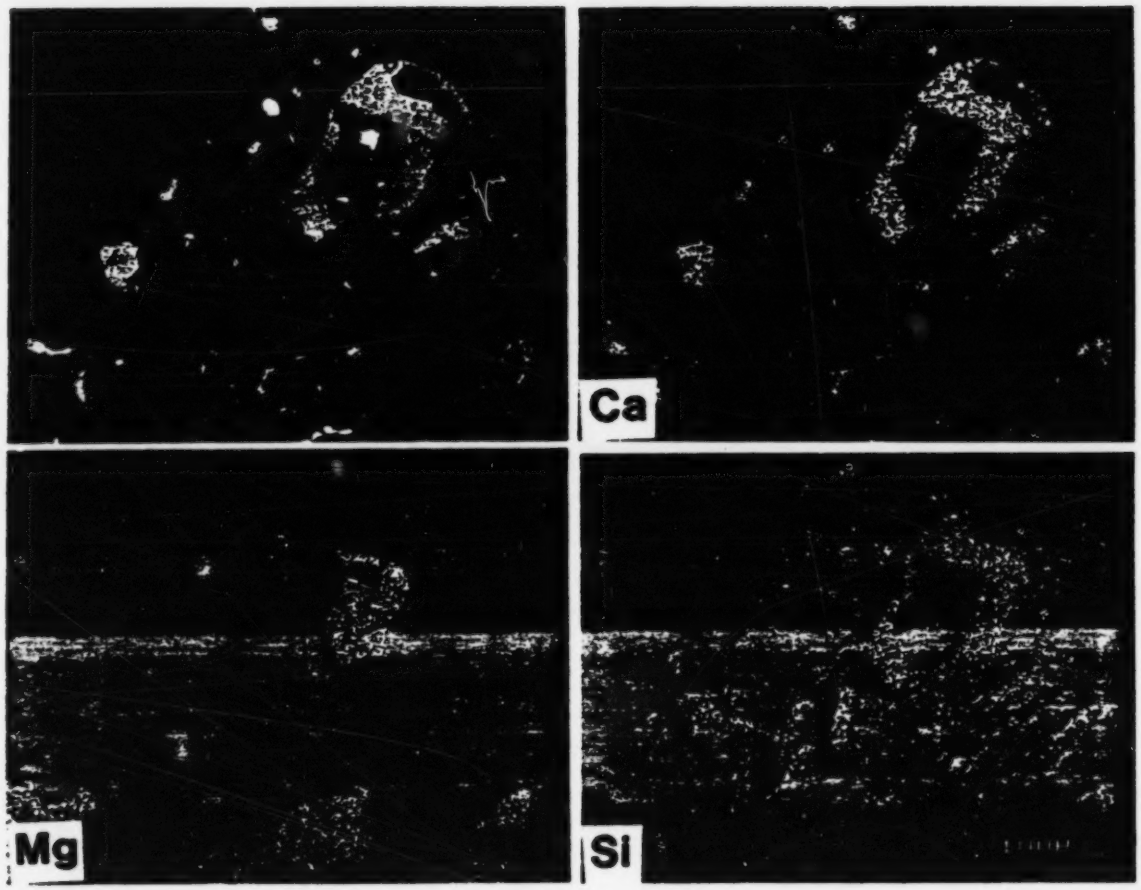

Fig. 18. SEM micrograph and elemental distribution maps of Ca, Mg and Si for MgO-C sample 6 in contact with slag of C/S = 3.54

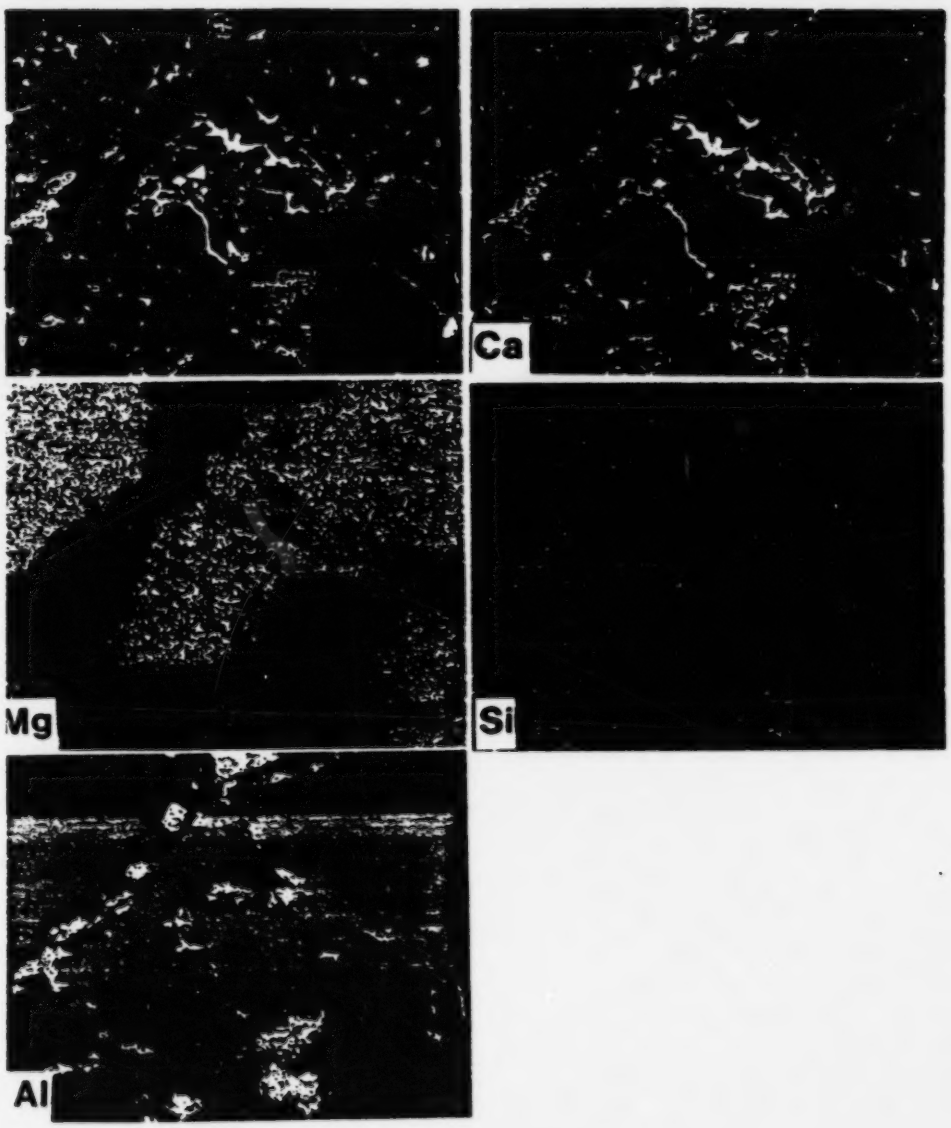

Fig. 19. SEM micrograph and elemental distribution maps of Ca, Mg, Si, and Al for MgO-C sample 7 in contact with slag of C/S = 3.54

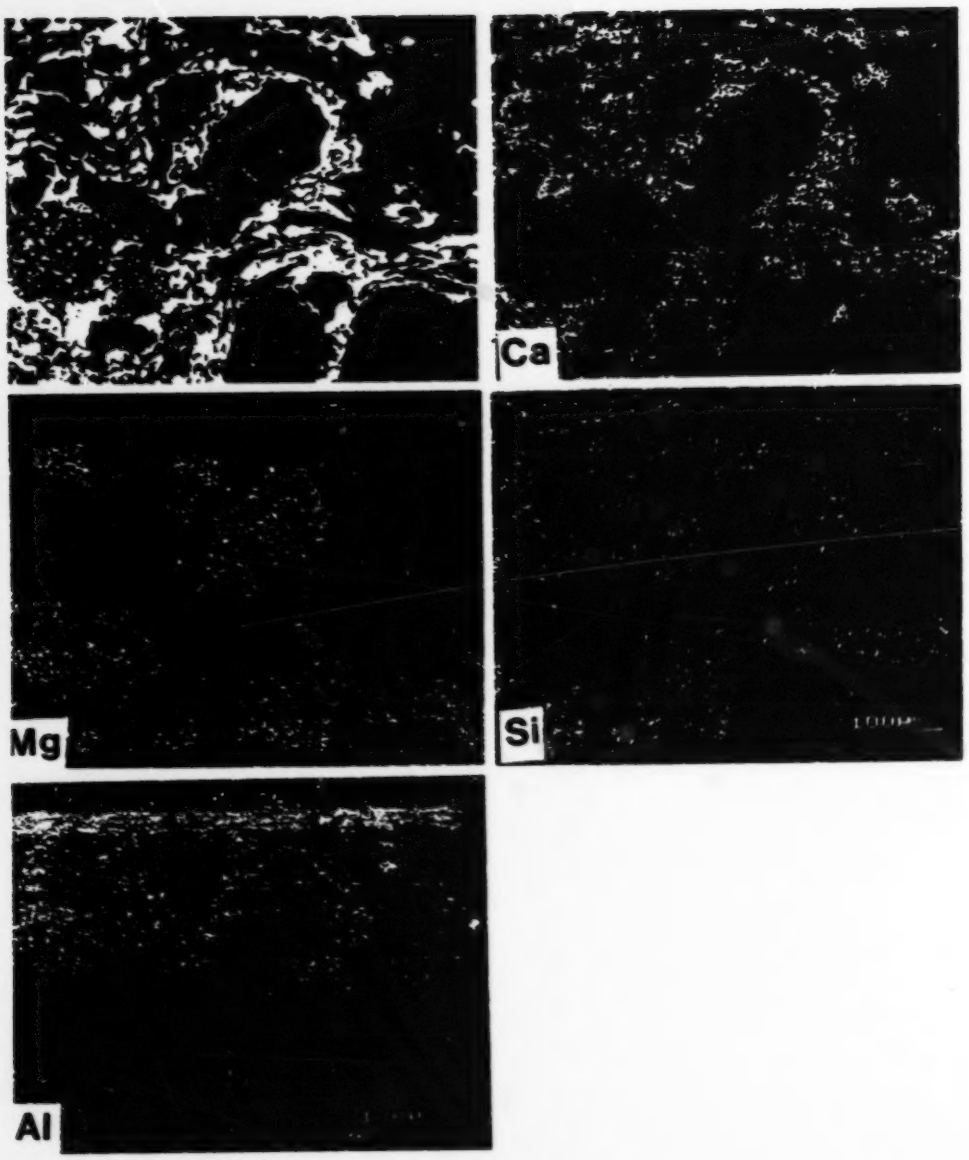

Fig. 20. SEM micrograph and elemental distribution maps of Ca, Mg, Si and Al for MgO-C sample 8B in contact with slag of C/S = 3.54

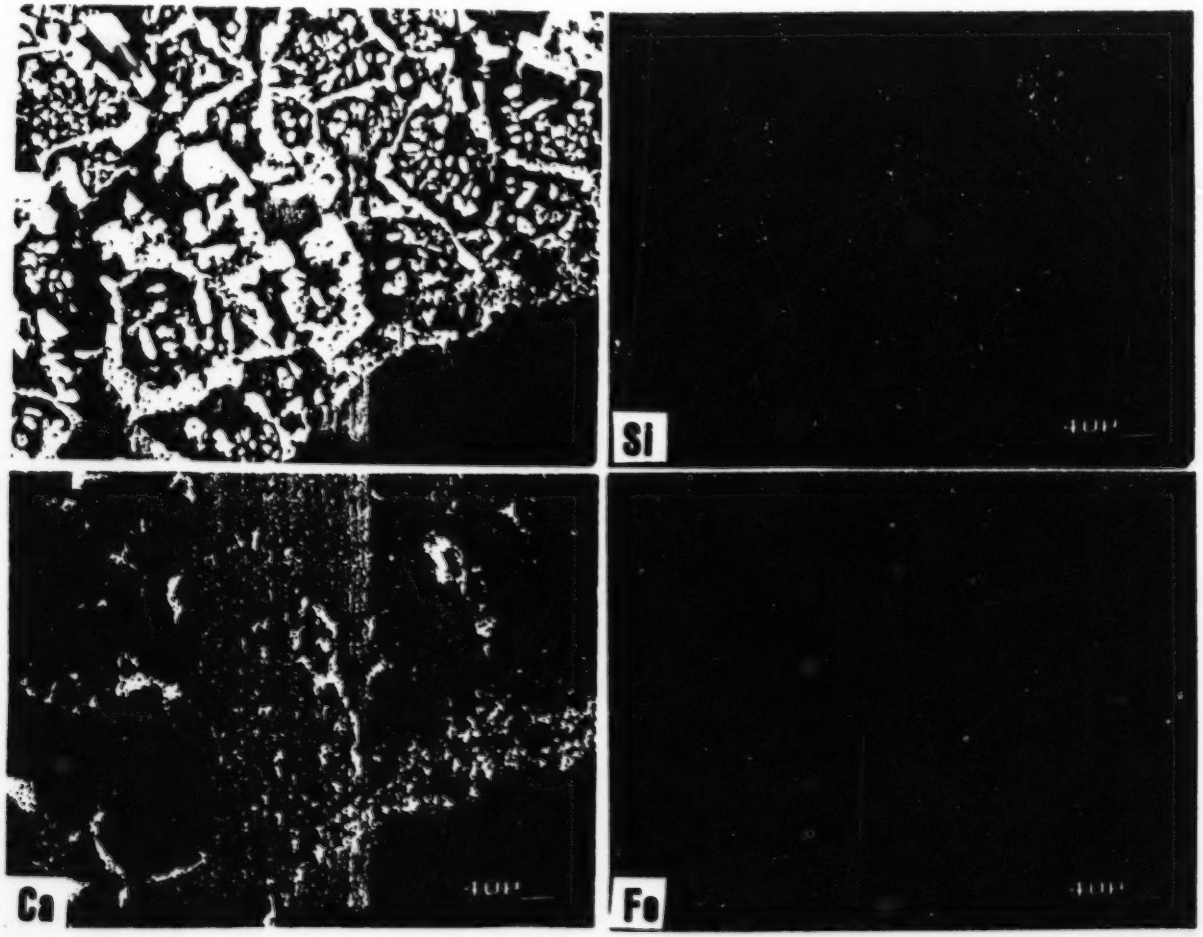

Fig. 21. SEM micrograph and EDXR maps for Ca, Si and Fe for fused cast chrome-magnesia brick in contact with slag of C/S = 1.35

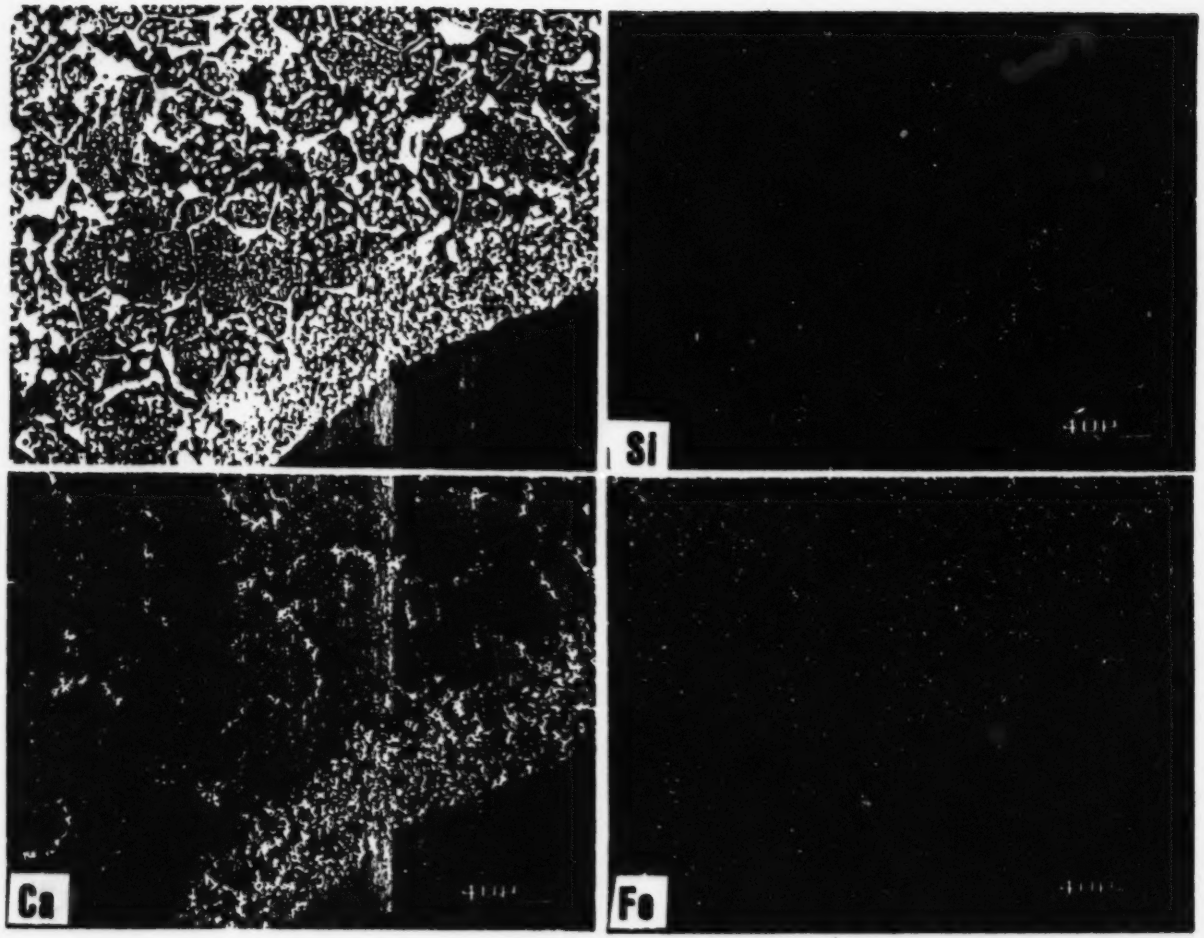

Fig. 22. SEM micrograph and elemental distribution maps of Ca, Si and Fe for fused cast chrome-magnesia in contact with slag of C/S = 3.54